

## Acoustic Coherent Backscatter Enhancement from Aggregations of Point Scatterers

David R. Dowling  
Department of Mechanical Engineering  
University of Michigan  
Ann Arbor, MI 48109-2133  
phone: (734) 936-0423 fax: (734) 764-4256 email: [drd@umich.edu](mailto:drd@umich.edu)

Award #: N00014-11-1-0258  
<http://www.personal.engin.umich.edu/~drd/>

### LONG-TERM GOALS

The overall long-term goal for this project is to determine if and how acoustic coherent backscatter enhancement (ACBE) can be used for classification of active sonar returns in a wide variety of ocean environments. During its first two years, this project has focused on simulations of acoustic multiple scattering from aggregations of omni-directional point scatterers to determine the parametric realms in which ACBE might be observed, and its characteristics when it is observed.

### OBJECTIVES

The detailed objectives of the current research effort are to determine the parametric dependence of ACBE peak amplitude, peak emergence rate as the number of observations increases, peak angular width, and peak time dependence. Here the independent parameters are the range between the scattering aggregation and the receiving array, the receiving array characteristics, incident wave characteristics (wave type, waveform, frequency, bandwidth, duration), and aggregation characteristics (scatterer cross section and mean spacing, overall aggregation size and shape, etc.). Eventually, underwater waveguide characteristics will be considered as well.

### APPROACH

The current approach involves numerical evaluation of the fundamental equations of multiple scattering from an aggregation of omni-directional point scatterers<sup>1</sup>. If  $\psi(\mathbf{r})$  is the harmonic acoustic pressure field at frequency  $\omega$  at the point  $\mathbf{r}$  and  $\psi_0(\mathbf{r})$  is the harmonic field incident on the aggregation of scatterers located at  $\mathbf{r}_n$ , then

$$\psi(\mathbf{r}) = \psi_0(\mathbf{r}) + \psi_s(\mathbf{r}) = \psi_0(\mathbf{r}) + \sum_{n=1}^N g_n \psi_n(\mathbf{r}_n) G(\mathbf{r}, \mathbf{r}_n), \quad (1)$$

where  $\psi_s(\mathbf{r})$  is the scattered field and is given by the sum in (1),  $N$  is the number of scatterers,  $g_n$  is the scattering coefficient of the  $n^{\text{th}}$  scatterer,  $\psi_n(\mathbf{r}_n)$  is the field incident on the  $n^{\text{th}}$  scatterer,

$$\psi_n(\mathbf{r}_n) = \psi_0(\mathbf{r}_n) + \sum_{j=1, j \neq n}^N g_j \psi_j(\mathbf{r}_j) G(\mathbf{r}_n, \mathbf{r}_j) \quad (2)$$

and  $G(\mathbf{r}_n, \mathbf{r}_j)$  is the free-space Green's function between the locations  $\mathbf{r}_n$  and  $\mathbf{r}_j$ ,

$$G(\mathbf{r}_n, \mathbf{r}_j) = \frac{\exp\{-ik_0|\mathbf{r}_n - \mathbf{r}_j|\}}{|\mathbf{r}_n - \mathbf{r}_j|} \quad (3)$$

where  $k_0 = \omega/c$  is the wave number magnitude of the incident field,  $c$  is the sound speed, and  $i = \sqrt{-1}$ . When the incident field and the scattering coefficients are known, (2) can be written  $N$  times, once for each scatterer  $1 \leq n \leq N$ , and these  $N$  algebraic equations can be solved to determine  $\psi_n(\mathbf{r}_n)$ . The total field at any location is then recovered from (1) and (3) using the known  $\psi_0(\mathbf{r})$ , the known  $g_n$ , and the calculated  $\psi_n(\mathbf{r}_n)$ . This formulation is akin to the direct boundary-integral formulation of computational acoustics with one computational element assigned to each scatterer. The computational burden of this approach is set by the inversion of the fully-populated  $N$ -by- $N$  algebraic system that determines  $\psi_n(\mathbf{r}_n)$ . In the current investigation, the scatterers are placed randomly with an average spacing  $s$ , and are identical without internal loss so the  $N$  scattering coefficients are all the same

$$g_n = g_1 = \left( \frac{\sigma_s}{4\pi} - \frac{k_0^2 \sigma_s^2}{16\pi^2} \right)^{1/2} - i \frac{k_0 \sigma_s}{4\pi}, \quad (4)$$

where  $\sigma_s$  is the scattering cross section. In the current investigations,  $\sigma_s$  is considered an independent parameter within the constraint imposed by conservation of acoustic energy:  $\sigma_s \leq 4\pi/k_0^2 = \lambda^2/\pi$ . For the current calculations, the incident field  $\psi_0(\mathbf{r})$  is a plane wave with amplitude  $A$  and wave number vector  $\vec{k}_0$ , and the backscatter direction ( $\phi = \varphi = 0$ ) is defined with respect to  $\vec{k}_0$  as shown in Figure 1. Rectangular aggregations of scatterers with width and depth dimensions  $h$  and  $w$  have been the primary geometry considered this fiscal year because this geometry readily allows both near-field and far-field investigations with a linear receiving array of length  $L$  when the number of scatterers is limited to a few thousand.

To search for the presence or absence of ACBE, the scattered field  $\psi_s(\mathbf{r})$  predicted by (1) is calculated at the elements of the receiving array, and aggregation-array distance  $R$  is varied to put the receiving array in the near-field, where the array's beam-steering angle  $\phi$  is relevant, or in the far-field of the aggregation, where the azimuthal scattering angle  $\varphi$  is relevant. For near-field calculations, the results are presented as  $B(\phi)/[B]_{ave}$  vs.  $\phi$ , where  $B(\phi)$  is the beamformed output of the receiving array, and  $[B]_{ave}$  is the array's average beamformed output in directions near backscatter but excluding the ACBE peak. For far-field calculations, the results are presented as  $|\psi(\varphi)|^2/|\psi_{ave}^2|$  vs.  $\varphi$ , where  $|\psi_{ave}^2|$  is the average mean-square pressure at that aggregation-receiver range in directions near backscatter but excluding the ACBE peak. The independent parameters of these investigations are  $A$ ,  $k_0$ ,  $\sigma_s$ ,  $s$ ,  $R$ ,  $L$ ,  $\phi$  or  $\varphi$ ,  $w$ , and  $h$ . Interestingly, the current problem can be stated in dimensionless terms by normalizing field values with the incident wave amplitude  $A$ , and by using wave number-scaled lengths. This reduces the number of independent parameters on which ACBE may depend from nine to seven.

The current focus of this research effort is on determining and understanding the parametric dependence of the ACBE peak's height and width on the seven dimensionless parameters ( $k_0\sqrt{\sigma_s}$ ,  $k_0s$ ,  $k_0R$ ,  $k_0L$ ,  $\phi$  or  $\varphi$ ,  $k_0w$ , and  $k_0h$ ), a task that has proved challenging. In particular, the current simulations show the ACBE peak enhancement may be 10 dB (or more) above the scattered intensity in other directions depending on the values of  $k_0\sqrt{\sigma_s}$  and  $k_0s$ . A maximum enhancement of 3 dB was expected based on prior theory<sup>2</sup>. Thus, understanding ACBE peak amplitude dependence on  $k_0\sqrt{\sigma_s}$ ,  $k_0s$  and aggregation shape has been the focus of this year's work. Investigations to date involving the remaining geometric parameters suggest they play more easily understood roles.

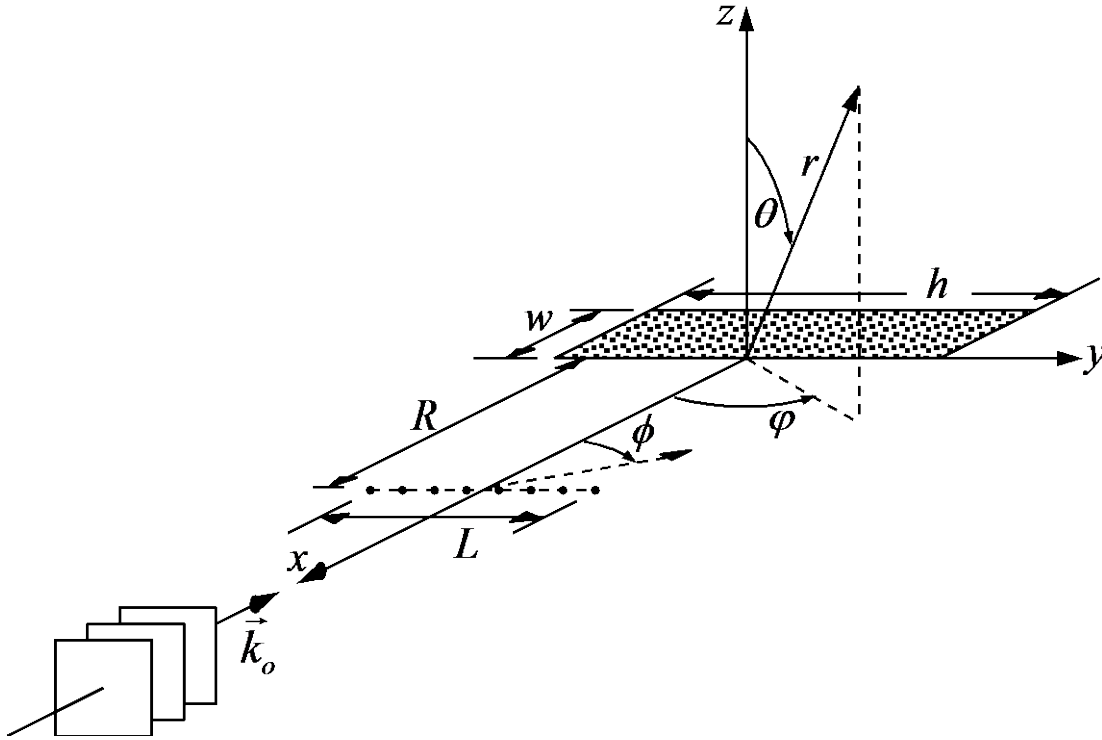


**Figure 1. Geometrical configuration of the multiple scattering simulations. A plane wave with amplitude  $A$  and wave number vector  $\vec{k}_0$  impinges on a rectangular aggregation of scatterers with dimensions  $w$  and  $h$ . Here  $\varphi$  is the scattering angle defined from the origin of coordinates, and  $\phi$  is the beam-steering angle defined from the broadside direction of the receiving array of length  $L$  that lies a distance  $R$  from the aggregation. The backscatter direction is  $\varphi = \phi = 0$ .**

These ACBE investigations are the current doctoral research of Ms. Adaleena Mookerjee. She is a US Citizen and a Ph.D. candidate.

In addition, an undergraduate team supported by NAVSEA through the Naval Engineering Education Center (NEEC) has developed a tank experiment (42" diameter, 42" depth, 16 receiving hydrophones) that may eventually be suitable for short-range ACBE experiments in the frequency range from 30 kHz to 120 kHz.

## WORK COMPLETED

The simulation code was subjected to three validation tests involving three different geometries. First acoustic energy conservation was checked for scattering from an aggregation of 1020 scatterers placed randomly within a sphere approximately five-wavelengths in diameter. For these simulations, the scatterers were strong,  $k_0\sqrt{\sigma_s} = 3.5$ , and relatively close to each other,  $k_0s = 2.5$ . When the incident plane wave is included the net acoustic power crossing a surface that encloses any aggregation of scatterers should be zero. The net power recovered from the simulations was 0.6% of the power scattered by one scatterer. Thus, the simulations are very nearly energy conserving.

Next, a linear arrangement of 13 evenly spaced scatterers was illuminated from the end-fire direction and the angles of maximum scattered intensity in the far-field of this linear aggregation were determined when  $k_0s = 8.38$  and  $16.8$ . The angles of increased scattered intensity recovered from the simulations successfully matched those determined from Bragg scattering formulae. Thus, the relative phasing of the scattered waves in the simulations appears to be correct.

The remaining simulation test involved comparing the simulation results with theory and experiments, and is described in the next section.

## RESULTS

Sample far-field ACBE simulation results are shown in Figure 2 for a cubical aggregation with a five-wavelength edge, 256 to 1024 Monte-Carlo trials,  $k_0\sqrt{\sigma_s} = 3.5$ , and four different average scatterer spacings:  $k_0s = 11.7, 5.5, 3.2,$  and  $2.5$ . Here, the vertical axis is  $\langle |\psi_s(R, \varphi)|^2 \rangle / \langle |\psi_s(R, \varphi)|^2 \rangle_{ave}$  and the horizontal axis is the far-field scattering angle  $\varphi$ . The  $\langle \rangle$ -brackets denote an ensemble average over Monte-Carlo trials. The central peak at  $\varphi = 0$  for  $k_0s = 3.2$  and  $2.5$  is produced by coherent backscattering enhancement. Interestingly, the enhancements shown by both peaks are well above the factor of two predicted and found in prior studies involving extended scattering media. Such greater-than-expected backscattering enhancement remains unexplained at the current time.

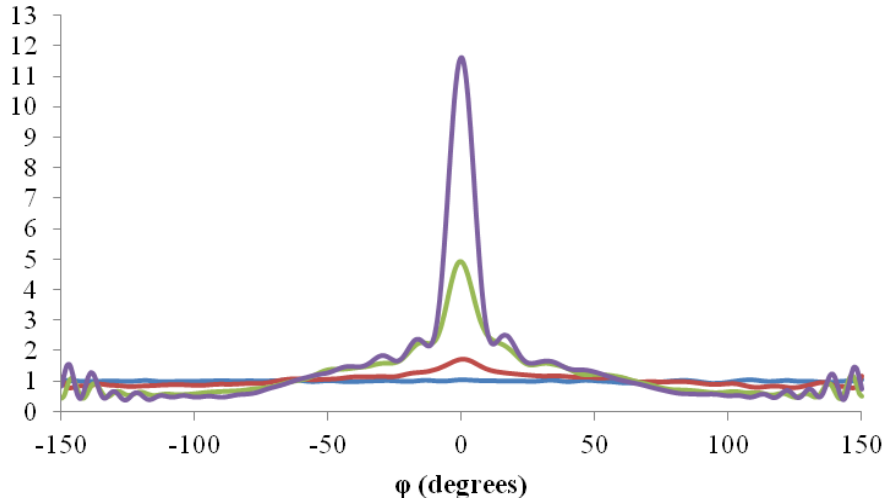


**Figure 2.** Mean-square scattered-field ratio  $\langle |\psi_s(R, \varphi)|^2 \rangle / \langle |\psi_s(R, \varphi)|^2 \rangle_{ave}$  vs. scattering angle  $\varphi$  for four different average scatterer spacings:  $k_0s = 11.7$  (blue),  $5.5$  (red),  $3.2$  (green), and  $2.5$  (purple). Here scatterers were placed in a cubical aggregation with 5 wavelength edges. The ensemble average was computed from 256 to 1024 Monte-Carlo trials. The acoustic coherent backscatter enhancement shown here for  $k_0s = 3.2$  and  $2.5$  is above that expected from prior optical and acoustic studies involving extended scattering media.

When the corners and edges of the cube are progressively removed, the ACBE peak amplitude decreases and the peak width mildly increases as the aggregation geometry becomes progressively more spherical. Figure 3 shows such results for  $k_{os} = 2.5$  and  $k_0\sqrt{\sigma_s} = 3.5$ . The vertical axis is  $\langle |\psi_s(R, \varphi)|^2 \rangle / \langle |\psi_s(R, \varphi)|^2 \rangle_{ave}$  and the horizontal axis is the far field scattering angle  $\varphi$ . The peak amplitude decreases as the aggregation becomes more spherical. The amplitude for the spherical aggregation (grey curve) is closest to the enhancement expected from prior studies.

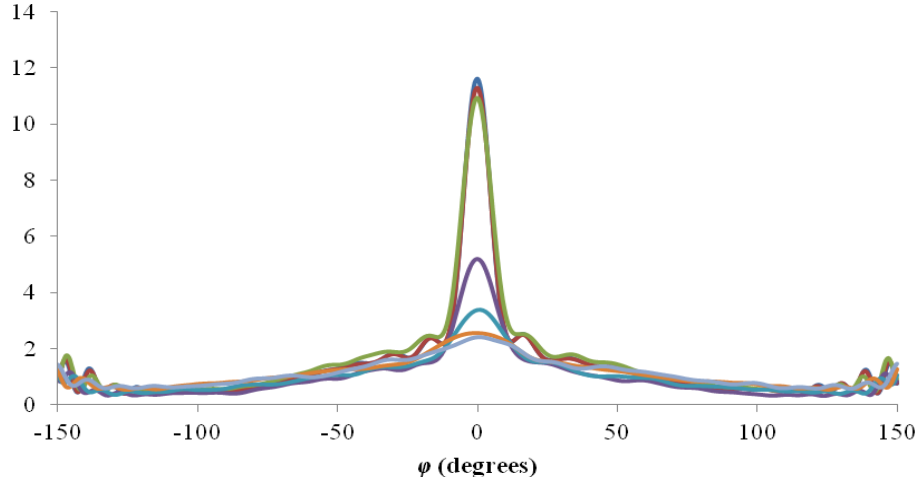


**Figure 3.** Mean square scattered-field ratio  $\langle |\psi_s(R, \varphi)|^2 \rangle / \langle |\psi_s(R, \varphi)|^2 \rangle_{ave}$  vs. scattering angle  $\varphi$  for an average scatterer spacing  $k_{os} = 2.5$ . Here scatterers are initially placed in cubical aggregation with a 5-wavelength edge (blue), and the corners and edges of the scattering aggregation are progressively removed by dropping scatterers beyond progressively smaller distances from the center of the aggregation. Results are shown when scatterers are dropped at distances greater than  $4\lambda$ , (red)  $3.7\lambda$ , (green)  $3.3\lambda$  (purple)  $3\lambda$  (light blue),  $2.7\lambda$  (orange) and  $2.5\lambda$  (gray). The amplitude of the peak at  $\varphi = 0$  decreases as the corners and edges of the scattering aggregation are removed.

As a further attempt to determine if these predictions are correct, the simulation geometry was adjusted to match a combination of parameters from two CBE experiments and then compared to relevant theoretical results. The scattering media parameters are obtained from an optics experiment<sup>3</sup> while the simulation geometry is that of an ultrasound experiment.<sup>4</sup> Both of these experiments need to be considered in order to accommodate the limitations associated with the current simulations. The optics experiment<sup>3</sup> utilized a small wavelength and a large number (trillions) of nominally-spherical scatterers in a three dimensional geometry. However, the current simulation cannot be completed for such a large number of scatterers. The ultrasound experiment<sup>4</sup> utilized a few thousand scatterers – a number that can be managed by the current simulations – but they were two-dimensional scatterers (vertical metallic rods). Wave scattering from such long cylinders is different than that from the omnidirectional point scatterers in the current simulations. So, in order to bridge the gap between optics and acoustics, the relevant scattering-medium length-scale ratios of the comparison simulations are obtained from the optics experiment while the scattering-aggregation and data-collection geometries are that of the ultrasound experiments.

These simulations were conducted using the geometry shown in Fig. 1 with the following parameters:  $k_0\sqrt{\sigma_s} = 0.232$ ,  $k_0s = 3.13$ ,  $k_0R = 131$ ,  $k_0L = 235$ ,  $k_0h = 293$ , and  $k_0w = 88$ . The solid line is the simulation result and the dashed line is the theoretical CBE result based on the mean-free path in the scattering medium. The results shown in this figure required: (i) fitting the mean-field intensity decay inside the scattering aggregation of the simulations to determine the mean free path, (ii) matching the scattering efficiency and spacing of the polystyrene spheres in the optics experiment to the simulation's point scatterers, and (iii) accounting for the finite angular resolution of the linear receiving array. Overall the match shown in Fig. 3 is good. The minor differences between the two curves are likely related to uncertainty in the fitting for the acoustic mean free path over the finite extent ( $w$  in Fig. 1) of the simulated scattering aggregation.

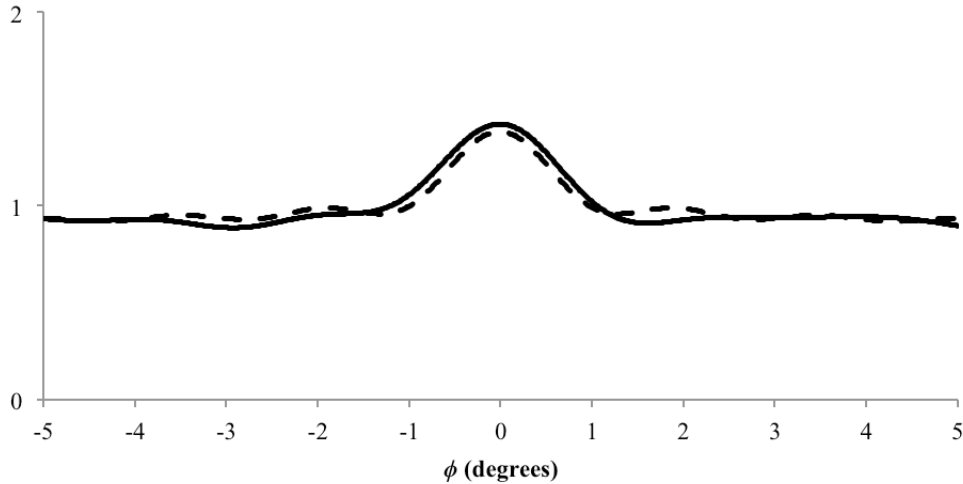


**Figure 4. Comparison of simulated and theoretical results for ACBE using a composite selection of experimental parameters. The vertical axis is  $B(\phi)/|B|_{ave}$  and the horizontal axis is the beam steering angle  $\phi$  shown in Fig. 1. The solid line is the simulation result. The dashed line is an evaluation of the relevant theory<sup>2</sup>. The minor differences between the two curves are likely related to uncertainty in determining the acoustic mean free path, a parameter in the theory that must be obtained by fitting the mean-field intensity decay inside the scattering aggregation of the simulations.**

Overall, these checks of the simulations have not yet found any deficiencies or errors. Thus, the greater-than-expected ACBE peak values may be genuine. However, an explanation for these high peak values has not yet been found, but the search continues and currently centers on possible coherent scattering and aggregation shape effects not included in CBE theory. A journal manuscript will be prepared when this explanation has been found.

## IMPACT/APPLICATION

In broad terms, this project ultimately seeks to determine if and how ACBE might be exploited for active sonar applications. In particular, if successful, it should prove useful for remote classification, because a large sonar return from a single large scatterer will likely not display ACBE while a similarly large sonar return from an aggregation of many small scatterers may display ACBE. Thus,

this research effort may eventually impact how active sonar signals are processed and displayed for tactical decision-making related to classification.

## **TRANSITIONS**

The results of this research effort should aid in the design of active sonar signal processors for tactical decision aids. However, at this time no direct transition links have been established with more applied research programs. Once the current simulation capability is more firmly established and validated, and promising results have been obtained, a transition path through NRL or one of the Navy's Warfare Centers will be sought.

## **RELATED PROJECTS**

This project is related the other projects funded under ONR's 2010 basic research challenge program. In particular, the work by Prof. Feuillade in Chile is most closely related.

## **REFERENCES AND PUBLICATIONS**

- [1] Foldy, L.L. (1945) "The multiple scattering of waves, I. General theory of isotropic scattering by randomly distributed scatterers," *Physical Review* Vol. 67, 107-119.
- [2] Akkermans, E., Wolf, P.E., and Maynard, R. (1986) "Coherent backscattering of light by disordered media: analysis of the peak line shape," *Physical Review Letters*, Vol. 56, No. 14, 1471-1474.
- [3] Wolf, P.-E., & Maret, G. (1985). Weak Localization and Coherent Backscattering of Photons in Disordered Media. *Physical Review Letters* Vol. 55, 2696-2699.
- [4] Aubry, A., Derode, A., Roux, P., & Tourin, A. (2007). Coherent backscattering and far-field beamforming in acoustics. *Journal of the Acoustical Society of America* Vol. 121, 70-77.

## **HONORS AND AWARDS**

Prof. Dowling was elected Fellow of the American Physical Society in November 2012.